Elaboration of high-transparency ZnO thin films by ultrasonic spray pyrolysis with fast growth rate

Sourav Bose, Christyves Chevallier, Sidi Ould Saad Hamady, David Horwat, Jean-François Pierson, Pascal Boulet, Thomas Gries, Thierry Aubert, Nicolas Fressengeas

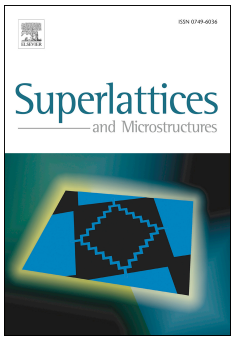

Elaboration of high-transparency ZnO thin films by ultrasonic spray pyrolysis with fast growth rate

Sourav Bose, Christyves Chevallier, Sidi Ould Saad Hamady, David Horwat, Jean-François Pierson, Pascal Boulet, Thomas Gries, Thierry Aubert, Nicolas Fressengeas

PII: S0749-6036(21)00143-9

DOI: https://doi.org/10.1016/j.spmi.2021.106945

Reference: YSPMI 106945

To appear in: *Superlattices and Microstructures*

Received Date: 3 February 2021

Revised Date: 12 May 2021

Accepted Date: 25 May 2021

Please cite this article as: S. Bose, C. Chevallier, S.O.S. Hamady, D. Horwat, Jean.-Franç. Pierson, P. Boulet, T. Gries, T. Aubert, N. Fressengeas, Elaboration of high-transparency ZnO thin films by ultrasonic spray pyrolysis with fast growth rate, *Superlattices and Microstructures* (2021), doi: https://doi.org/10.1016/j.spmi.2021.106945.

Graphical Abstract

Elaboration of high-transparency ZnO thin films by ultrasonic spray pyrolysis with fast growth rate

Sourav Bose,Christyves Chevallier,Sidi Ould Saad Hamady,David Horwat,Jean-François Pierson,Pascal Boulet,Thomas Gries,Thierry Aubert,Nicolas Fressengeas

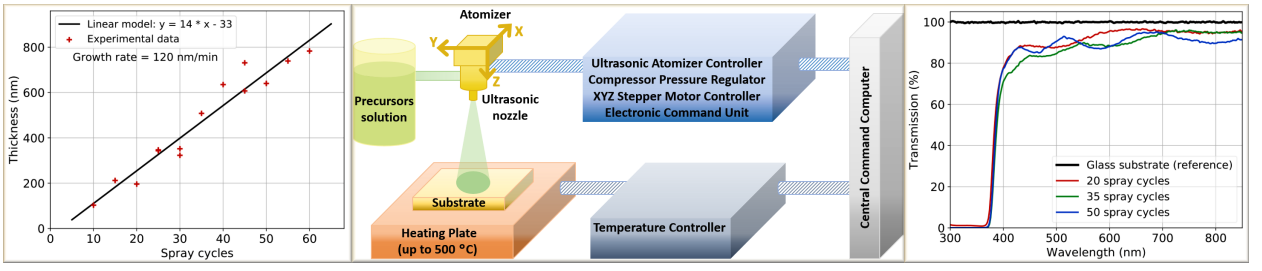

Highlights

Elaboration of high-transparency ZnO thin films by ultrasonic spray pyrolysis with fast growth rate

Sourav Bose,Christyves Chevallier,Sidi Ould Saad Hamady,David Horwat,Jean-François Pierson,Pascal Boulet,Thomas Gries,Thierry Aubert,Nicolas Fressengeas

- Fast growth rate of ZnO thin films using ultrasonic spray pyrolysis
- High transparency in a wide range of thickness from 100 nm up to 800 nm
- c-axis preferred orientation with large grain size and minimized defects
- Fulfill criteria for use in applications such as all-oxide solar cells

Elaboration of high-transparency ZnO thin films by ultrasonic spray pyrolysis with fast growth rate

Sourav Bose[a], Christyves Chevallier[a], Sidi Ould Saad Hamady[a,*], David Horwat[b], Jean-François Pierson[b], Pascal Boulet[b], Thomas Gries[b], Thierry Aubert[a] and Nicolas Fressengeas[a]

[a] *Université de Lorraine, CentraleSupélec, LMOPS, F-57000 Metz, France.*
[b] *Université de Lorraine, CNRS, IJL, F-54000 Nancy, France.*

ARTICLE INFO

Keywords:
Ultrasonic Spray Pyrolysis
Zinc Oxide
Thin-Film
Transparency
Growth Rate
All-Oxide Solar Cell

ABSTRACT

In this work, ZnO films are deposited by the ultrasonic spray pyrolysis technique on soda lime glass substrates by following a specific design of experiment. The ZnO films are spray deposited using different elaboration parameters. Optical, morphological, structural and electrical properties of the ZnO films are systematically investigated. Fourier-transform infrared and transmittance spectra are measured to examine their optical properties. They are correlated to their structural properties determined by X-ray diffraction and Raman spectroscopy. The surface morphology is analyzed using atomic force microscopy while the electrical conductivity is measured using the four probe technique. This comprehensive analysis shows that ZnO thin films elaborated using ultrasonic spray pyrolysis with fast growth rate have a high transparency in a wide thickness range, making them suitable for use in applications such as all-oxide solar cells.

1. Introduction

Elaboration techniques used for the growth of ZnO thin films are mainly based on reactive sputtering [1, 2], pulsed laser deposition [3, 4], sol-gel [5], molecular beam epitaxy [6], and spray pyrolysis [7–12]. The improved technique of ultrasonic spray pyrolysis allows for a better control of the deposition compared to conventional pneumatic spray systems. Indeed, spraying an aerosol with an ultrasonic nozzle increases not only the yield of atoms actually deposited on the substrate surface, but also the uniformity and quality of the elaborated thin films. Ultrasonic spray pyrolysis is thus more suitable for uniform deposition on a large area and can be up-scaled for high production yield with roll to roll processing, while keeping accurate coating formation at an optimized cost [9, 13–17]. One of the main applications of ZnO is in the emerging all-oxide solar cells technology. This technology is entirely based on metal oxide semiconductors, which become attractive since they allow for the design of devices based only on non-toxic, stable and earth-abundant elements. Cu_2O/ZnO p-n heterojunctions thin films are the most studied solar cells based on metal oxides, in which cuprous oxide (Cu_2O) is used as the absorber material and zinc oxide (ZnO) as the window layer [18, 19]. Beyond photovoltaic applications, ultrasonic spray pyrolysis ZnO is used for applications in the field of photocatalysis [15, 16, 20], surface acoustic wave sensors [17], as well as for solar-blind ultraviolet photodetectors and light emitting diodes [3, 6, 9, 21, 22]. In all these applications, very high optical and structural properties of the film alongside with a fast growth rate, compatible with low-cost production, and typically a wide range of thickness values, usually between 50 nm and 800 nm, need to be achieved.

In this article, the focus is set on comprehensive study of the ZnO thin films elaborated with an in-house optimized ultrasonic spray pyrolysis technique with respect to the elaboration parameters, as described in section 2. Section 3 presents the optical and morphological properties of the ZnO thin films that we elaborated and the analysis of their structural properties.

*Corresponding author
thumbnails/sas_email.jpeg (S. Ould Saad Hamady)
ORCID(s): 0000-0002-6449-3321 (S. Bose); 0000-0002-0480-6381 (S. Ould Saad Hamady); 0000-0001-7938-7647 (D. Horwat); 0000-0001-8790-3162 (J. Pierson); 0000-0003-0684-4397 (P. Boulet); 0000-0003-4601-2675 (T. Gries); 0000-0001-5148-770X (T. Aubert); 0000-0002-5534-712X (N. Fressengeas)

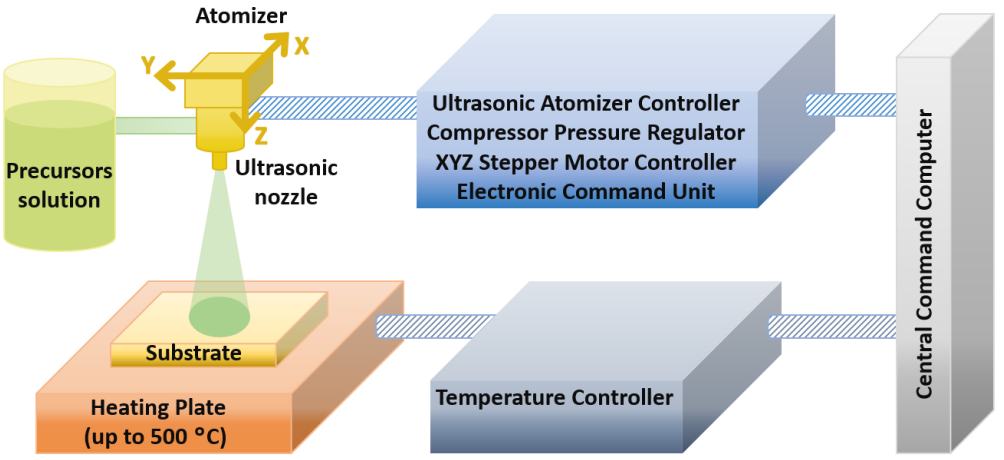

Figure 1: Schematic diagram of the ultrasonic spray pyrolysis system used for the elaboration of ZnO thin films.

2. Elaboration and characterization procedure

In this experimental work, ZnO thin films were prepared by ultrasonic spray pyrolysis and characterized using a large set of optical, morphological and structural techniques.

2.1. Ultrasonic spray process

Elaboration is done using an ExactaCoat system from Sono-Tek with an Accumist ultrasonic nozzle operating at 120 kHz. A schematic view of this system is displayed in figure 1. The precursor solutions are obtained by dissolving zinc acetate dihydrate (Merck 108802) in deionized water at a concentration before adjusting the pH with acetic acid (Alfa Aesar 10994-AE). The soda lime glass substrates were ultrasonically cleaned in different solutions such as acetone, isopropanol and distilled water for 15, 10 and 5 minutes, respectively to remove organic residues, and were maintained at a fixed temperature between 350 °C and 450 °C prior to and during d eposition. The substrate holder is equipped with thermocouple, heating elements and a high-stability temperature controller. The precursor solution is vaporized with the 120 kHz ultrasonic generator. The precursor solution is atomized with a nozzle-to-substrate distance of 10 cm. The resulting aerosol is then guided towards the substrate by a controlled air flow, at a relative pressure of about 13.8 kPa, in the ambient atmosphere. As the aerosol nears the heated substrate, the droplets vaporize and the precursors are adsorbed onto the surface to undergo a pyrolytic reaction to form the zinc oxide thin film as shown in equation 2, with a possible formation of zinc hydroxide $Zn(OH)_2$.

Pyrolysis of zinc acetate on the heated substrate :

$$Zn(CH_3COO)_2 + 4\,O_2 \rightarrow ZnO + 4\,CO_2\uparrow + 3\,H_2O\uparrow \quad (1)$$

Formation of zinc hydroxide :

$$Zn(CH_3COO)_2 + 2\,H_2O \rightarrow Zn(OH)_2 + 2\,CH_3COOH\uparrow \quad (2)$$

2.2. Design of experiment

In order to investigate the effect of all the impacting ultrasonic spray pyrolysis parameters, we set up a design of experiment to systematically characterize the thin films properties with respect to the main elaboration parameters:

a. the spray number of cycles that we varied from 10 to 60. This parameter fixes the duration of each elaboration.
b. the spray flow rate, ranging from 0.3 mL/min to 0.7 mL/min.
c. the concentration of precursor solution varying from 0.03 mol/L to 0.10 mol/L.
d. the precursor solution pH was set from 4 to 5.
e. the deposition temperature, varying from 350 °C to 450 °C.

Each spray parameter was varied while keeping the other parameters fixed. The reproducibility of the ultrasonic spray pyrolysis process was systematically certified by regularly elaborating, at least three times, each sample with a given combination of the parameters below. The other parameters such as the nozzle height and the scan speed were fixed to obtain high transparency thin films with fast growth rate in a wide thickness range.

2.3. Characterizations

The thickness of the elaborated ZnO films was systematically measured at 3 points at the centre of the spray zone, using a Bruker Dektak XT profilometer. Their optical properties were obtained through transmission measurements with a UV-VIS-NIR Perkin-Elmer Lambda 900 spectrometer in the wavelength range of 300-850 nm with a 2 nm resolution step at room temperature. The absorption coefficient α of a ZnO film was derived from its transmittance T by the Beer-Lambert relationship: $\alpha = (1/d)\, log\,(1/T)$, where d is its thickness. The optical bandgap energy is then calculated using the Tauc model for direct bandgap materials in the high absorption region: $\alpha\, h\nu = A\sqrt{h\nu - E_g}$, where $h\nu$ is the photon energy, A is a constant and E_g is the optical bandgap. For sub-bandgap photon energy, the absorption coefficient of ZnO layers shows the Urbach tail which is related to crystalline lattice disorder in the thin films. It is expressed as $\alpha = \alpha_0 \exp\left(h\nu/E_u\right)$, where E_u is the Urbach energy and α_0 a constant. The values of the Urbach energy of the ZnO thin films was obtained from the inverse of the slope of $\log(\alpha)$ versus photon energy ($h\nu$).

The crystal structure and growth orientation analysis of the ZnO films were carried out using X-ray diffraction (XRD Bruker D8 Advance) with $Cu - K\alpha$ radiation of $\lambda = 0.15406$ nm. Raman spectrometry was performed as well to understand the structural properties using an excitation wavelength of 532 nm under $z(y-)\bar{z}$ configuration, thanks to the LabRAM Aramis system from Horiba Jobin-Yvon. In order to perform a quantitative study of the effect of the deposition parameters on the thin film structure, the structural properties are estimated from the XRD diffractograms through the following physical parameters.

First, the lattice parameters a and c are evaluated from the definition of the interplanar spacing d for a given (hkl) crystallographic plane in the hexagonal wurtzite crystal structure:

$$d_{hkl} = \left(\frac{4}{3a^2}\left(h^2 + k^2 + hk\right) + \frac{l^2}{c^2}\right)^{-1/2} \tag{3}$$

The d spacing being calculated by using the standard Bragg's equation and peak position from the diffractograms.

Secondly, to determine the crystallite size, we used a modified Scherrer method developed by Monshi *et al.* in [23] and demonstrated to be more accurate than using the standard Scherrer formula:

$$D = \frac{K\,\lambda}{\beta\, cos\,(\theta)} \tag{4}$$

where λ is the X-ray wavelength, β the angular line width at full width at half maximum, θ the Bragg's angle and K the Scherrer constant taken to be equal to 0.9. $\lambda = 0.15406$ nm in our case.

In this modified Scherrer method, all the identified peaks are used to estimate the crystallite size by linearly fitting $ln(\beta)$ against $ln(1/cos(\theta))$ and taking the value of D from its intercept.

Lastly, the texture factor $F_{(xyz)}$ is obtained for the (xyz) diffraction plane using the following equation [24]:

$$F_{(xyz)} = \frac{I^{exp}_{(xyz)}/I^{ref}_{(xyz)}}{\frac{1}{N}\sum I^{exp}_{(hkl)}/I^{ref}_{(hkl)}} \tag{5}$$

where $I^{exp}_{(xyz)}/I^{ref}_{(xyz)}$ is the integrated peak intensity ratio between the experimental and reference data corresponding to the (xyz) diffraction plane of study; $I^{exp}_{(hkl)}/I^{ref}_{(hkl)}$ is the integrated peak intensity ratio between the experimental and reference data for each (hkl) diffraction plane; and N the number of (hkl) diffraction planes chosen as N = 4 to match the diffracting planes (100), (002), (101) and (110). The maximal value of F is N = 4. The XRD reference used for the structural analysis of the experimental thin films is chosen from the RRUFF project database and corresponds to a randomly oriented polycrystalline ZnO powder (RRUFF ID: R060027.1) [25].

FTIR measurements on thin films were performed with a commercial Agilent FTIR 680 spectrometer in attenuated total reflection (ATR) mode. Spectra were acquired in the range of $600 - 4000\ cm^{-1}$ with a spectral resolution

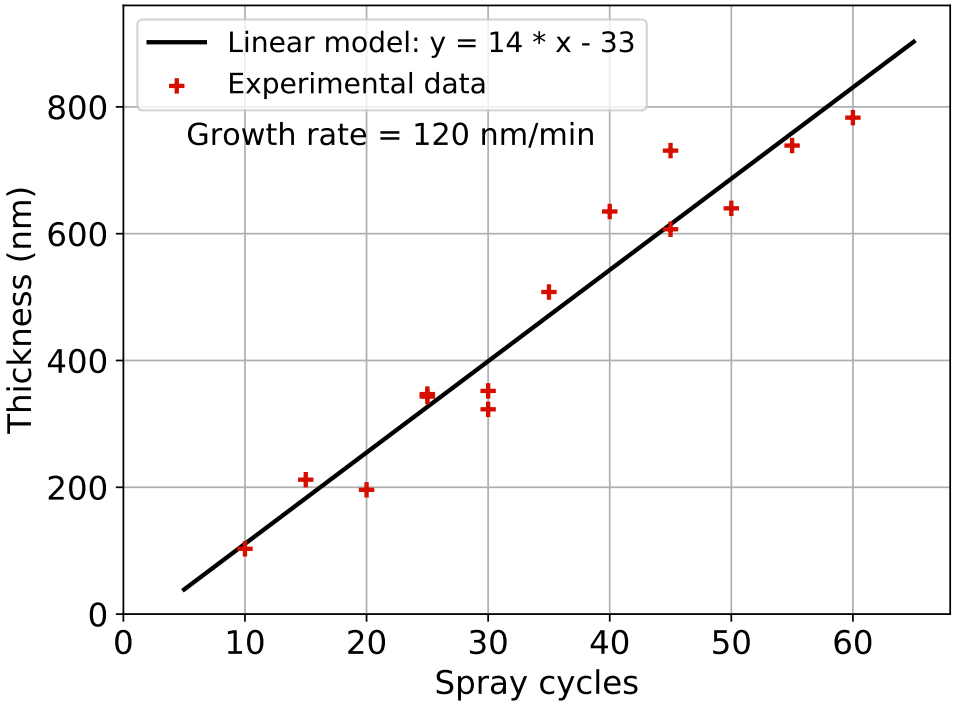

Figure 2: Relation between the ZnO film thickness and the number of spray cycles is shown along with a linear fit. For 25, 30 and 45 cycles, two measurements on two samples are shown, to assess the process stability. One spray cycle corresponds to about 7 seconds and the growth rate is about 120 nm/min (i.e. 14 nm/cycle).

of 4 cm^{-1}. Reference spectra were acquired before each acquisition to determine the absorption spectra in ambient conditions. Each measurement was averaged over 200 scans in continuous mode to improve the signal-to-noise ratio.

The topography of the ZnO films was examined in resonant mode using a Nano-Observer atomic force microscope developed by CSInstruments. Annealing in ambient air was performed at 300 °C during 30 minutes and then the film conductivity was determined using a home-made four probe technique.

3. Results and discussion

The samples elaborated by ultrasonic spray pyrolysis using the design of experiment (section 2.2) were investigated using various characterization techniques in order to understand the effect of the elaboration parameters on their optical, morphological and structural properties and to reach for the requirements of the photovoltaic application.

The thickness was systematically measured at three points of the spray zone and then averaged. The relation between the ZnO film thickness and the number of spray cycles is shown in figure 2. It is seen that the growth of the ZnO films is linear with respect to the number of spray cycles. The fitted line does not cross the origin indicating that there is an incubation time at the very first stage of the growth, where grains coalesce and grow to form the ZnO thin film. This nucleation/coalescence time is usually observed in the spray pyrolysis and sol-gel processes [26–28]. The reproducibility and the stability of the process was checked by elaborating several samples (up to four) in the same process and by regularly elaborating new samples with the same previously used conditions. The growth rate was about 120 nm/min corresponding to 14 nm per spray cycle. From this calibration, we fixed the number of spray cycles to 20, corresponding to a ZnO thickness of about 200 nm as a typical value for application in all-oxide solar cells. This growth rate of about 120 nm/min was obtained with thickness ranging from about 100 nm up to almost 800 nm. In literature, Kenanakis *et al.* [15] reports growth rate of 1 nm/min, Mata *et al.* [16] reaches up to 42 nm/min in their process, Ergin *et al.* [14] could reach 55 nm/min and recently Ynineb *et al.* [29] reaches a growth rate of 80 nm/min in their spray process. We could maintain this high growth rate along with high nozzle scan speed and a good

	Deposition temperature (°C)	Precursor concentration (mol/L)	Texture factor $F_{(002)}$	Crystallite size (nm) ± 5 nm	Lattice parameters c ; a (nm) ± 0.00010 nm
	450	0.03	1.96	35	0.51896 ; 0.32418
	450	0.05	2.48	39	0.51905 ; 0.32417
	450	0.10	0.83	21	0.51955 ; 0.32379
	400	0.10	0.45	15	0.52227 ; 0.32513
	350	0.10	0.18	16	0.52434 ; 0.32532
ZnO powder [25]	—	—	1.00	—	0.52074 ; 0.32503
ZnO/Glass [9]	400	—	—	25	0.51980 ; 0.31830
ZnO/Glass [30]	300 (cycles)	[0.03 ; 0.10]	[1.60 ; 2.60]	[12 ; 17]	—
ZnO/Glass [31]	[365 ; 465]	[0.03 ; 0.20]	—	[2 ; 4]	—
ZnO/Glass [32] ultrasonic spray	[350 ; 450]	0.10	—	[13 ; 18]	0.52100 ; 0.32480
ZnO/Glass [33]	450 (anneal. 1h)			[7 ; 33]	0.52109 –
ZnO/Glass [34] spin-coating	500 (anneal. 2h)	—	—	[19 ; 23]	0.52098 ; 0.32387
ZnO/Sapphire [35]	room temperature			[27 ; 52]	0.52620 –
ZnO/Si [36] RF sputtering	id.	—	—	—	– 0.32527
ZnO/Quartz [37]	550			24	0.51460 –
ZnO/Sapphire [38] pulsed laser deposition	675	—	—	21	—

Table 1
The measured crystallographic data with respect to the deposition temperature and precursor solution concentration. For all samples, the flow rate was fixed to 0.5 mL/min; the precursor solution pH was fixed to 4 and the number of spray cycles was fixed to 20. The value of the texture coefficients $F_{(002)}$ and crystallite size are estimated using the procedure described in section 2.3. Are also shown the data of the ZnO powder (RRUFF ID: R060027.1) [25] used as reference for the texture analysis. State-of-the-art results are also displayed, as a single value or a range of values, alongside with the deposition technique and temperature.

repeatability.

3.1. Structural properties

The structural properties of the sprayed ZnO films were analyzed following the experimental procedure described in section 2.3, using X-ray diffraction (XRD) and Raman spectroscopy, in order to identify the deposited material structure and to study its crystalline quality.

The X-ray diffractograms of the deposited ZnO thin films are shown in figures 3a and 3b. Diffractograms show four ZnO peaks for the (100), and (002), (101) and (110) planes attributed to hexagonal wurtzite phase with space group $P6_3mc$. X-ray diffractograms exhibit a Lorentzian shape that is usually attributed to a size induced broadening of the peaks while the strain induced broadening is better modeled by a Gaussian or Voigt functions [39]. Other parameters such as stoichiometry and defects have an impact on the X-ray peak shape. To precisely determine peaks position and full width at half maximum, a least squares fitting procedure was used.

The texture coefficient and the crystallite size are calculated and summarized in table 1 alongside with the state-of-the-art results for various deposition methods. The calculated lattice parameters values are very close to the values $a = 0.32503$ nm and $c = 0.52074$ nm for pure and stoichiometric ZnO taken from the RRUFF database, as shown in the table.

The crystallite sizes, calculated using the modified Scherrer method described in 2.3, vary between 15 nm to 39 nm with maximum obtained for a deposition temperature of 450 °C and a precursor solution concentration of 0.05 mol/L.

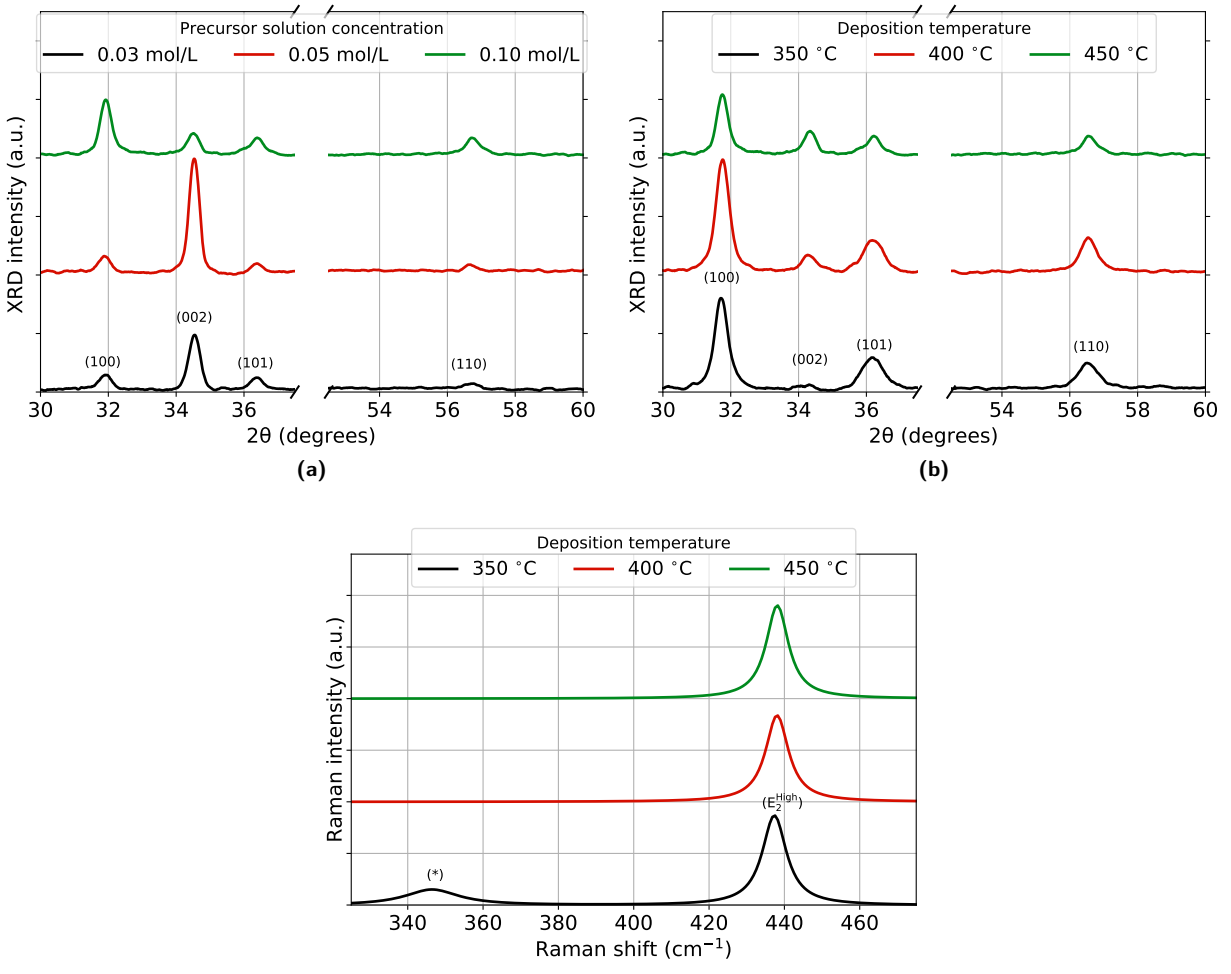

Figure 3: 3a & 3b: XRD diffraction patterns for ZnO thin films grown on soda lime glass substrates. Unless specified otherwise, the deposition temperature is fixed to 450 °C; the number of spray cycles is set to 20; the spray flow rate is 0.5 mL/min; the solution concentration is fixed to 0.10 mol/L and the precursor solution pH is 4; **3c**: Lorentzian fits of the Raman spectra with different deposition temperatures. The E_2^{High} Raman vibrational mode was identified at $\approx$ 438 cm^{-1}. The peak marked (*) at $\approx$ 350 cm^{-1} is not identified as related to ZnO.

This value is higher than values obtained very recently in similar deposition conditions by de Godoy *et al.* [30] and comparable or superior to similar thin films reported in literature, as shown in table 1.

Finally, the study of the effect of deposition temperature and precursor solution concentration on the thin film texture is then performed. The high value of $F_{(002)}$ for a deposition temperature of 450 °C and precursor solution concentration of 0.03 mol/L and 0.05 mol/L suggests that the growth occurs preferentially with the (002) orientation plane parallel to the substrate in these conditions. These results are in agreement with the recently reported results [30, 40], where it is suggested that ZnO films with c-axis orientation has minimum surface energy with uniform oriented crystallites with low defects and trapping sites.

At a higher precursor solution concentration of 0.10 mol/L or at lower deposition temperatures (350 °C and 400 °C), the $F_{(002)}$ values are close or lower than unity which indicates that the growth has no longer a (002) preferential orientation perpendicular to the substrate plane.

To complete the XRD structural analysis of the thin films, Raman spectroscopy was performed on samples elab-

Temperature (°C)	Precursor concentration (mol/L)	Precursor pH (±0.1)	Flow rate (mL/min)	Average transmission (%)	Bandgap (eV) ±0.01 eV	Urbach (meV) ±5 meV
450	0.10	4.0	0.5	93.5	3.26	63
450	0.10	4.0	0.3	95.4	3.28	69
450	0.10	4.0	0.7	80.0	3.29	67
450	0.03	4.0	0.5	91.5	3.28	77
450	0.05	4.0	0.5	90.0	3.26	78
400	0.10	4.0	0.5	79.9	3.28	84
350	0.10	4.0	0.5	68.3	3.26	96
450	0.10	5.0	0.5	80.3	3.26	77

Table 2
The spray elaboration parameters along with the measured parameters extracted from figures 4a, 4b, 4c and 4d. The number of spray cycles was set to 20.

orated at temperatures of 350 °C, 400 °C and 450 °C as shown in figure 3c. From the fitting of the spectra with a Lorentzian function, the main peak at a Raman shift of 438 cm^{-1} is identified as the E_2^{High} ZnO Raman phonon vibration of the wurtzite structure for all samples. In addition, another broad peak appears at a Raman shift around 350 cm^{-1} for the lowest deposition temperature of 350 °C. This peak was not identified as the ($E_2^{High} - E_2^{Low}$) ZnO mode, usually observed in ZnO [41], since its position and width are too different from the observed values for this ZnO mode. From the broad nature of this peak and the change of texture observed from the XRD patterns in the previous paragraph, the peak origin is tentatively attributed to a defect-related mode in the disordered ZnO layers originating from incomplete spray pyrolytic reaction at lower temperatures. To validate this hypothesis, further investigations are conducted and detailed in the next section 3.2. It is worth noting that at low deposition temperature the E_2^{High} peak full width at half maximum is about 8 cm^{-1}, value consistent with the values usually reported for ZnO thin films deposited by sputtering [42].

3.2. Optical properties and morphology

The optical properties and the morphology of the ZnO films were investigated with respect to the deposition parameters in order to analyze the transparency of the thin films. These properties were studied using the transmission measurements and completed with FTIR spectroscopy and atomic force microscopy to investigate the origin of the observed variation in the structural properties.

The transmittance spectra are plotted in figure 4a with respect to the spray flow rate, in figure 4b with the precursor solution concentration, in figure 4c with deposition temperature and in figure 4d with pH at values of 4 and 5. In all the cases the number of spray cycles was fixed to 20, as it is seen from figure 2 that with this spray cycles value, we can achieve ZnO film thickness of approximately 200 nm which is compatible to the use as window layer for new solar cells and, in particular, in all-oxide photovoltaic structures, while higher ZnO thickness is compatible for use as TCO contact. The spray elaboration parameters that are fixed and varied during the spray are detailed in table 2 along with the measured parameters.

Figures 4a, 4b, 4c and 4d and table 2 allow to infer that a notable loss of transparency happens when the flow rate is too high which is well correlated to the variation in the structural properties observed in section 3.1, when the substrate temperature is reduced below 450 °C and when pH of precursor solution is increased. Indeed, with a high flow rate, the quantity of material deposited is very high which contributes to incomplete pyrolysis process. With a reduced substrate temperature as suggested by Silva *et al.* in [43], the pyrolysis reaction is incomplete and tends to form zinc hydroxide $Zn(OH)_2$, as shown in equation 2. The oxygen–zinc stoichiometry plays also an important role and could explain the loss of transparency for the highest value of the spray flow rate as evidenced in ZnO thin films elaborated by DC sputtering [35, 44, 45]. Indeed, films deposited with a high spray flow rate could exhibit a relatively

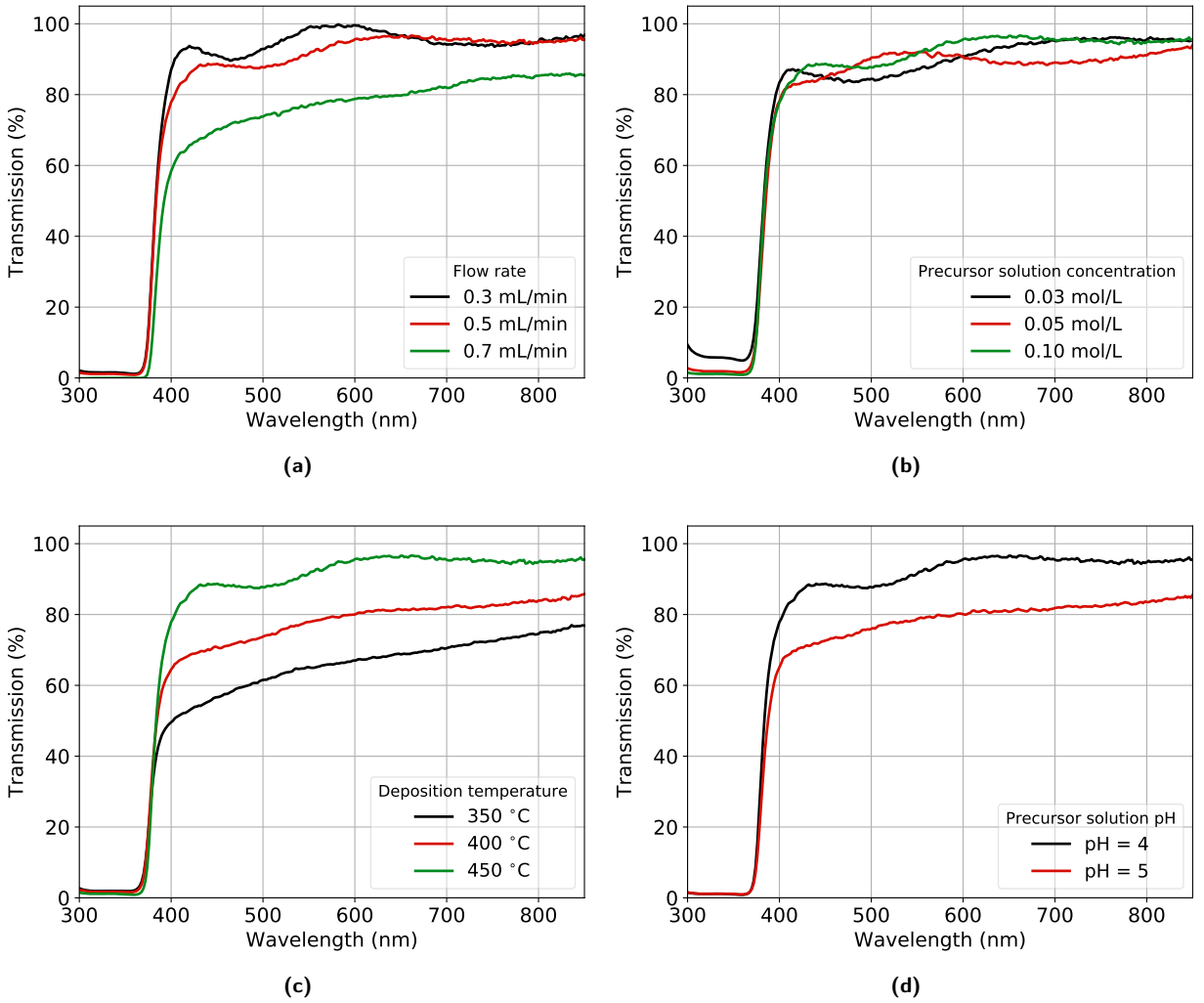

Figure 4: Transmission spectra for ZnO thin films grown on soda lime glass substrates as functions of growth parameters. Unless specified otherwise, the flow rate is set to 0.5 mL/min; the deposition temperature is fixed to 450 °C; the number of spray cycles is set to 20; the solution concentration is fixed to 0.10 mol/L and the pH is set to 4. The spray parameters are detailed in table 2.

high ratio of Zn/O, as observed in reactively-sputtered films when the oxygen gas flow rate decreases. The effect of the incomplete pyrolysis reaction and the Zn/O ratio is expected to impact the growth mechanism and thus the surface morphology which can explain the observed variation in the thin films transparency.

On figure 5a are presented the optical transmission spectra for ZnO films, grown with three different spray cycle numbers, at a substrate temperature of 450 °C, with a flow rate of 0.5 mL/min of a precursor solution concentration of 0.10 mol/L and pH 4.

Figure 5b shows the plots of $(\alpha\, h\nu)^2$ versus the photon energy $h\nu$. The values of the optical bandgap and the Urbach energies corresponding to the transmittance measurements shown in figure 5b are presented in table 3 alongside with the state-of-the-art values. These values are extracted from the experimental data according to the procedure detailed in section 2.3. It is seen that the average transmission, taken for wavelengths between 400 nm and 800 nm, remains in the [90–95]% range, for thicknesses ranging from $\approx$ 200 nm up to 640 nm and compares well with the results found in literature for ZnO thin films. The low values of Urbach energy, below 72 meV, suggest improvement of optical quality of the films during the spray growth, in agreement with the studies in [40, 46]. The usually reported

	Deposition temperature (°C)	Spray cycles	Thickness (nm) ±10 nm	Average transmission (%)	Bandgap (eV) ±0.01 eV	Urbach (meV) ±5 meV
	450	20	196	93.5	3.28	63
	450	35	508	92.4	3.25	72
	450	50	640	90.6	3.26	61
ZnO/Glass [9]	400			86	3.25	
ZnO/Glass [40]	400			[84 ; 90]	3.24	
ZnO/Glass [31]	[365 ; 465]	—	—	[83 ; 91]	[3.35 ; 3.40]	—
ZnO/Glass [32] ultrasonic spray	[350 ; 450]			85	[3.29 ; 3.31]	
ZnO/Sapphire [50] e-beam	600	—	—	—	—	[74 ; 99]
ZnO/Glass [33] spin-coating	annealing 1h 450	—	—	84	[3.24 ; 3.33]	—
ZnO/Si [36] RF sputtering	room temperature	—	—	[80 ; 92]	[3.24 ; 3.29]	—
ZnO/Quartz [37]	550			—	3.34	—
ZnO/Glass [51] pulsed laser deposition	300	—	—	70	3.83	120

Table 3
The values of thickness, transmission, optical bandgap and Urbach energy with respect to the spray number of cycles. The precursor concentration set to 0.10 mol/L; the precursor pH set to 4; and the flow rate set to 0.5 mL/min. State-of-the-art results are also displayed, as a single value or a range of values, alongside with the deposition technique and temperature.

transmission average value is in the [80–85]% range [7–9, 13, 21, 47] in the visible spectrum region with some works recently report transmittance as high as 95 % for layers of thickness below 30 nm elaborated using a custom made spray pyrolysis and CVD system [10] and 90% for ultrasonic spray pyrolysis elaborated layers [12]. An annealing step can increase the transmittance beyond 90 % as shown in [48]. In our spray elaboration process we were able to produce ZnO films with average transmission of up to 95% in the visible spectrum region without a post-annealing process. This is mostly possible because of an effective control of the spray parameters following a precise design of experiment. Noticeably, the shaping air pressure, the nozzle-substrate distance, the number of spray cycles, the solution concentration and the temperature are very important to have excellent atomization so that the deposition is conformal with complete pyrolytic reaction.

After obtaining highly transparent ZnO thin films, the electrical properties were determined using the four probes technique. Samples deposited at 450 °C with optimal solution concentration of 0.05 mol/L, spray flow rate of 0.5 mL/min, number of cycle of 50 and a pH of 4 were analyzed after a post annealing at 300 °C for 30 minutes. A measured average resistivity of 1.5 $\Omega \times$ cm was obtained after annealing while all deposited films were highly resistive before annealing. The post-annealing resistivity is comparable to a recently measured values in similar conditions by Edinger *et al.* [49] for non-intentionally doped ZnO deposited by spray pyrolysis.

To assess the morphology of the ZnO films, atomic force microscopy (AFM) measurements were done at resonant mode with a frequency of 323 kHz. 3D micrographs were captured and shown in figure 6. The micrographs reveal a granular and polycrystalline morphology with increase in the grain size for ZnO when spray is done at a higher temperature. The grain size observed from the surface micrographs analysis, about 40 nm for the mean grain diameter, is consistent with the crystallite size deduced from X-ray diffraction analysis. The most uniform ZnO surface is obtained for a pH 4 solution and a 450 °C substrate temperature. Grain agglomerates can indeed be noticed for lower temperatures or for a pH 5 solution. The formation of these agglomerates could be the result of the formation of hydroxides associated to an incomplete spray pyrolytic reaction. Furthermore, the high 450 °C growth temperature also leads to a more uniform surface because it contributes to reducing the surface mechanical stress. Similar temperature effects were reported in the AFM study by Prasada Rao *et al.* [21]. The RMS roughness obtained for the ZnO thin films

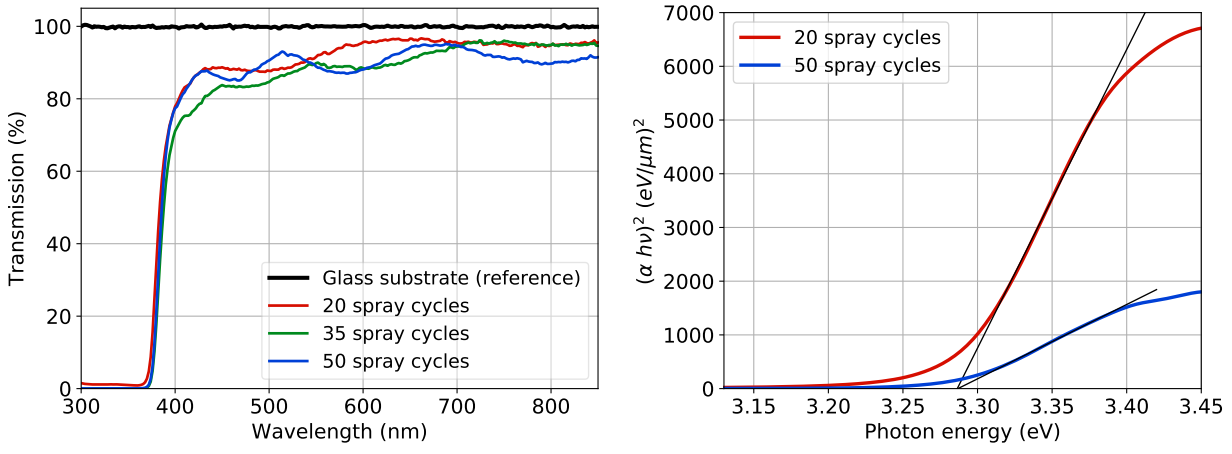

Figure 5: 5a Transmission spectra for ZnO thin films grown on soda lime glass substrates with different spray cycles; 5b Tauc plots of ZnO thin films with two different spray cycles.

deposited with ultrasonic spray pyrolysis at 450 °C from a pH 4 solution compares well with values usually measured for ZnO films obtained by more complex techniques such as ion-beam or RF magnetron sputtering [52, 53].

To investigate on the presence of O-H in the ZnO films, Fourier Transform Infrared Spectroscopy (FTIR) analysis was done. The analysis is in accordance with previous studies [54, 55]. The spectra shown in figures 7a and 7b reveal the presence of bands assigned to the oscillating vibrations O-H ($\approx$ 3400 cm^{-1}), symmetric and asymmetric valency bands C-H ($\approx$ 3000 cm^{-1}, 1500 cm^{-1}) and stretching vibrations Zn-OH ($\approx$ 1400 cm^{-1}) and Zn-O ($\approx$ 900 cm^{-1}). As expected, the presence of O-H bands is more intense for the ZnO sprayed at lower substrate temperature and the one sprayed with pH = 5 of precursor solution. This behavior is well correlated to the formation of agglomerates observed using AFM and could be the result of the formation of hydroxides associated to an incomplete spray pyrolytic reaction. It goes well with the studies of Edinger *et al.* [13] and Li *et al.* [56], where it is suggested that acetic acid in the precursor solution helps to reduce the precipitation of $Zn(OH)_2$. Indeed, adding acetic acid permits the ionization of zinc acetate and the subsequent reaction, with the formation of $ZnCH_3COO^+$, prevents the formation of zinc hydroxide precipitates, as follows:

$$\begin{aligned} &CH_3COOH \leftrightarrow CH_3COO^- + H^+ \\ &Zn^{2+} + CH_3COO^- \leftrightarrow ZnCH_3COO^+ \end{aligned} \tag{6}$$

4. Conclusions

Highly transparent thin films at fast growth rate were obtained with smooth enough surface morphology, high grain size with low agglomeration. The measured optical and structural parameters compare well with the literature values obtained using more complex techniques such as ion-beam or RF magnetron sputtering. Low Urbach energies suggests high ZnO crystalline quality. Very high transparency is noted for most samples with values above 90 % with a maximum at about 95 %. The measured electrical resistivity is comparable to the measured values in similar conditions for non-intentionally doped ZnO. In addition, FTIR spectroscopy was conducted to assess the presence of O-H bands, which could account for incomplete pyrolysis reaction hindering the transparency. XRD structural investigations reveal the polycrystalline nature of the ZnO thin films, with a (002) preferential orientation for the optimized spray elaboration parameters. The level of crystallization of the films is quite high with crystallite sizes reaching up to 39 nm with a texture and c-axis preferential orientation. Raman analysis confirms the hexagonal wurtzite structure of the crystals with a high intensity E_2^{High} peak. Future work will focus on the control of the ZnO films electrical properties through a doping that allows to keep high transparency and good crystalline quality.

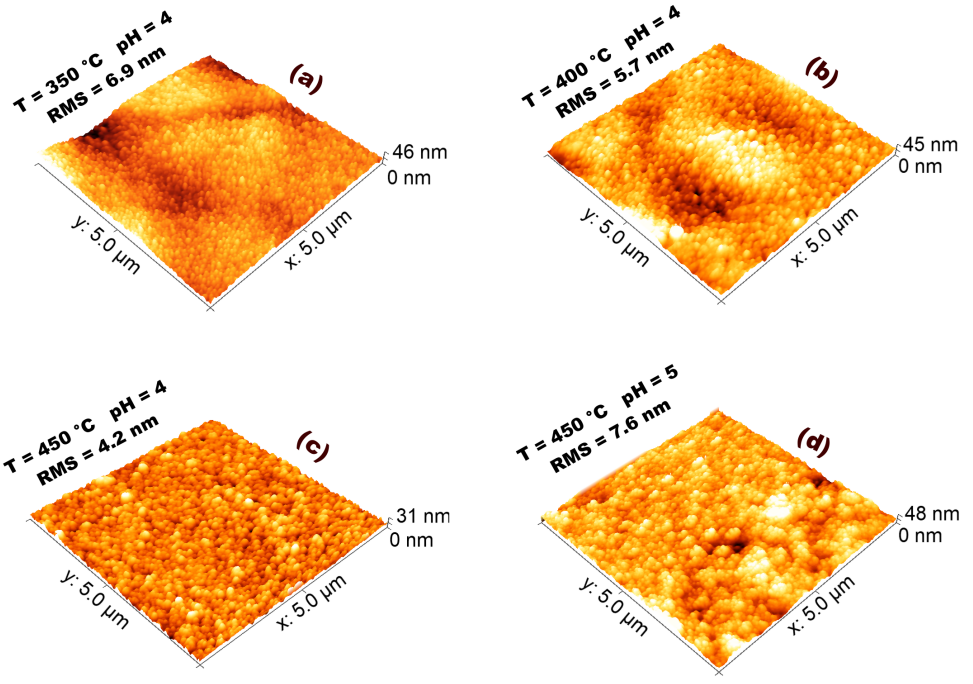

Figure 6: AFM 3D micrographs for ZnO thin films grown on soda lime glass substrate at **(a)** substrate temperature of 350 °C during spray and precursor solution pH = 4 with a root mean square (RMS) roughness of 6.9 nm; **(b)** substrate temperature of 400 °C and precursor solution pH = 4 with RMS = 5.7 nm; **(c)** substrate temperature of 450 °C and precursor solution pH = 4 with RMS = 4.2 nm; **(d)** substrate temperature of 450 °C and precursor solution pH = 5 with RMS = 7.6 nm.

Conflict of interest

The authors declare no conflict of interest.

Acknowledgments

This research was supported by “AAP mi-lourd – CentraleSupélec”, “Pôle M4 – Université de Lorraine”, “CPER MatDS”, “Partenariats Hubert Curien (PHC) Hibiscus” and “Lorraine Université d’Excellence (LUE)” in the framework of the “HECTOR” research project. The authors gratefully acknowledge Queny Kieffer from the CAREL Platform of the LMOPS laboratory. They also gratefully acknowledge Dr. Thomas Kauffmann from the Spectroscopy Platform of the LMOPS laboratory and Jordan Maufay for his help in conducting the XRD measurements.

References

[1] Y Yan, R Lim, and J M White. High mobility amorphous zinc oxynitride semiconductor material for thin film transistors. *Journal of Applied Physics*, 106(7):074512, 2009. doi: 10.1063/1.3236663.

[2] H K Yadav, K Sreenivas, and V Gupta. Study of metal/ZnO based thin film ultraviolet photodetectors: The effect of induced charges on the dynamics of photoconductivity relaxation. *Journal of Applied Physics*, 107(4):044507, 2010. doi: 10.1063/1.3291133.

[3] C Jin, A Tiwari, and R J Narayan. Ultraviolet-illumination-enhanced photoluminescence effect in zinc oxide thin films. *Journal of Applied Physics*, 98(8):083707, 2005. doi: 10.1063/1.2108156.

[4] C Bundesmann, N Ashkenov, M Schubert, D Spemann, T Butz, EM Kaidashev, M Lorenz, and M Grundmann. Raman scattering in ZnO thin films doped with Fe, Sb, Al, Ga, and Li. *Applied Physics Letters*, 83(10):1974–1976, 2003. doi: 10.1063/1.1609251.

[5] Y S Kim, W P Tai, and S J Shu. Effect of preheating temperature on structural and optical properties of ZnO thin films by sol–gel process. *Thin Solid Films*, 491(1):153–160, 2005. ISSN 0040-6090. doi: 10.1016/j.tsf.2005.06.013.

[6] H Liu, V Avrutin, N Izyumskaya, U Ozgur, and H Morkoc. Transparent conducting oxides for electrode applications in light emitting and absorbing devices. *Superlattices and Microstructures*, 48(5):458–484, 2010. doi: 10.1016/j.spmi.2010.08.011.

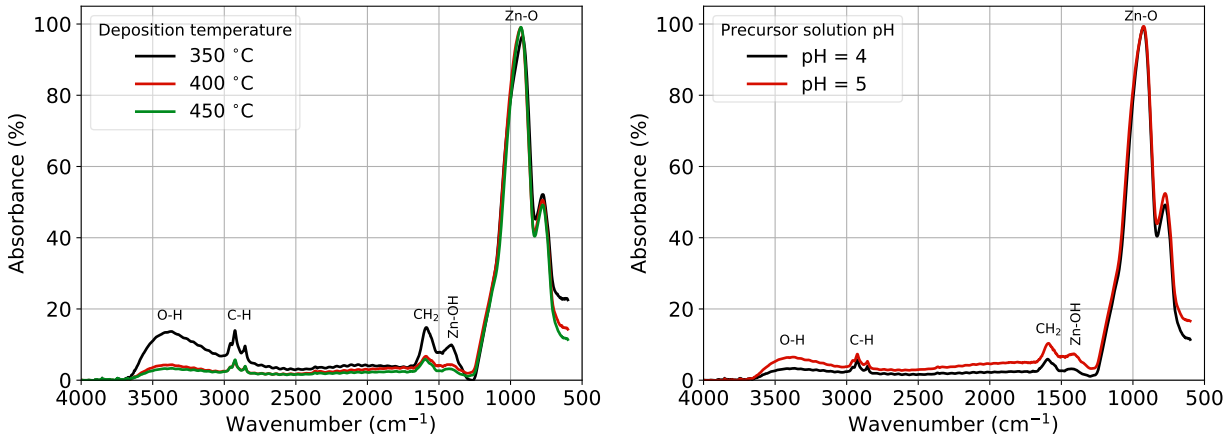

Figure 7: FTIR spectra for ZnO thin films grown on soda lime glass substrates at different temperatures. Unless specified otherwise, the number of spray cycles was fixed to 20; the spray flow rate was fixed to 0.5 mL/min; the solution concentration was fixed to 0.10 mol/L; the deposition temperature was fixed to 450 °C; and its pH was fixed to 4. Are identified the following vibrations: O-H ($\approx$ 3400 cm^{-1}); C-H ($\approx$ 3000 cm^{-1}, 1500 cm^{-1}); Zn-OH ($\approx$ 1400 cm^{-1}) and Zn-O ($\approx$ 900 cm^{-1}).

[7] F D Paraguay, W L Estrada, D R Acosta, E Andrade, and M Miki-Yoshida. Growth, structure and optical characterization of high quality ZnO thin films obtained by spray pyrolysis. *Thin Solid Films*, 350(1):192–202, 1999. ISSN 0040-6090. doi: 10.1016/S0040-6090(99)00050-4.

[8] N Kalyani, Y C Ching, and N Azizi. Structural and optical properties of ZnO thin films obtained by spray pyrolysis. *Materials Research Innovations*, 18(sup6):126–130, 2014. doi: 10.1179/1432891714Z.0000000001013.

[9] P Singh, A Kumar, X Deepak, and D Kaur. Growth and characterization of ZnO nanocrystalline thin films and nanopowder via low-cost ultrasonic spray pyrolysis. *Journal of Crystal Growth*, 306(2):303–310, 2007. doi: 10.1016/j.jcrysgro.2007.05.023.

[10] Chandan Biswas, Zhu Ma, Xiaodan Zhu, Toshiyuki Kawaharamura, and Kang L Wang. Atmospheric growth of hybrid ZnO thin films for inverted polymer solar cells. *Solar Energy Materials and Solar Cells*, 157:1048–1056, 2016.

[11] Alexander G Fedoseev, Natalia A Lashkova, and Lev B Matyushkin. Zno and aluminium doped ZnO thin films synthesis by ultrasonic spray pyrolysis technique. In *2017 IEEE Conference of Russian Young Researchers in Electrical and Electronic Engineering (EIConRus)*, pages 1391–1393. IEEE, 2017.

[12] H Mokhtari, M Benhaliliba, A Boukhachem, MS Aida, and YS Ocak. Nanostructured device based on coated ZnO layer as a window in solar cell applications. *Materials Science Poland*, 36(4):570–583, 2018.

[13] S Edinger, J Bekacz, M Richter, R Hamid, R Wibowo, A Peic, and T Dimopoulos. Influence of the acetic acid concentration on the growth of zinc oxide thin films prepared by spray pyrolysis of aqueous solutions. *Thin Solid Films*, 594:238–244, 2015. doi: 10.1016/j.tsf.2015.04.027.

[14] B Ergin, E Ketenci, and F Atay. Characterization of ZnO films obtained by ultrasonic spray pyrolysis technique. *International Journal of Hydrogen Energy*, 34:5249–5254, 2009. doi: 10.1016/j.ijhydene.2008.09.108.

[15] G Kenanakis and N Katsarakis. Ultrasonic spray pyrolysis growth of ZnO and ZnO:Al nanostructured films: Application to photocatalysis. *Materials Research Bulletin*, 60:752–759, 2014. doi: 10.1016/j.materresbull.2014.09.060.

[16] V Mata, A Maldonado, and M Olvera. Deposition of ZnO thin films by ultrasonic spray pyrolysis technique. effect of the milling speed and time and its application in photocatalysis. *Materials Science in Semiconductor Processing*, 75:288–295, 2018.

[17] Y Lee, H Kim, and Y Roh. Deposition of ZnO thin films by the ultrasonic spray pyrolysis technique. *Japanese Journal of Applied Physics*, 40:2423–2428, 2001. doi: 10.1143/JJAP.40.2423.

[18] M G Kohan, I Concina, and A Vomiero. All-oxide solar cells. In *Solar Cells and Light Management*, pages 229–246. Elsevier, 2020.

[19] G Korotcenkov. *The Future of Semiconductor Oxides in Next-Generation Solar Cells*. Elsevier, 2017.

[20] M K Singha, A Patra, V Rojwal, K G Deepa, and D Kumar. Ultrasonic spray pyrolysis deposited ZnO thin film for photocatalytic activity. *AIP Conference Proceedings*, 2082(1):030023, 2019. doi: 10.1063/1.5093841.

[21] T Prasada Rao and M C Santhoshkumar. Effect of thickness on structural, optical and electrical properties of nanostructured ZnO thin films by spray pyrolysis. *Applied Surface Science*, 255(8):4579–4584, 2009. ISSN 0169-4332. doi: 10.1016/j.apsusc.2008.11.079.

[22] J Agrawal, T Dixit, A I Palani, M S R Rao, and V Singh. Zinc interstitial rich ZnO honeycomb nanostructures for deep UV photodetection. *Physica Status Solidi (RRL)–Rapid Research Letters*, 12(10):1800241, 2018.

[23] A Monshi, M R Foroughi, M R Monshi, et al. Modified scherrer equation to estimate more accurately nano-crystallite size using XRD. *World journal of nano science and engineering*, 2(3):154–160, 2012.

[24] D Ariosa, F Elhordoy, E A Dalchiele, R E Marotti, and C Stari. Texture vs morphology in ZnO nano-rods: On the x-ray diffraction characterization of electrochemically grown samples. *Journal of Applied Physics*, 110(12):124901, 2011. doi: 10.1063/1.3669026.

[25] R T Downs. The RRUFF Project: an integrated study of the chemistry, crystallography, Raman and infrared spectroscopy of minerals. In *Program and Abstracts of the 19th General Meeting of the International Mineralogical Association in Kobe, Japan, 2006*, 2006.

[26] A Palafox, G Romero-Paredes, A Maldonado, R Asomoza, D R Acosta, and J Palacios-Gomez. Physical properties of CdS and CdS:In thin films obtained by chemical spray over different substrates. *Solar energy materials and solar cells*, 55(1-2):31–41, 1998.

[27] K Murakami, K Nakajima, and S Kaneko. Initial growth of SnO2 thin film on the glass substrate deposited by the spray pyrolysis technique. *Thin Solid Films*, 515(24):8632–8636, 2007.

[28] M W Zhu, J H Xia, R J Hong, H Abu-Samra, H Huang, T Staedler, J Gong, C Sun, and X Jiang. Heat-activated structural evolution of sol-gel-derived ZnO thin films. *Journal of Crystal Growth*, 310(4):816–823, 2008.

[29] F Ynineb, D E Guitoume, D Mendil, N Attaf, M S Aida, and H Farh. ZnO nanorods prepared by ultrasonic spray pyrolysis: Effect of deposition time on the structural morphological and optical properties. In *Defect and Diffusion Forum*, volume 397, pages 88–100. Trans Tech Publ, 2019.

[30] M P F de Godoy, L K S de Herval, A A C Cotta, Y J Onofre, and W A A Macedo. ZnO thin films design: the role of precursor molarity in the spray pyrolysis process. *Journal of Materials Science: Materials in Electronics*, pages 1–12, 2020.

[31] N Kumari, S R Patel, and J V Gohel. Optical and structural properties of ZnO thin films prepared by spray pyrolysis for enhanced efficiency perovskite solar cell application. *Optical and Quantum Electronics*, 50(4):180, 2018.

[32] T Prasada Rao, M C Santhosh Kumar, A Safarulla, V Ganesan, S R Barman, and C Sanjeeviraja. Physical properties of ZnO thin films deposited at various substrate temperatures using spray pyrolysis. *Physica B: Condensed Matter*, 405(9):2226–2231, 2010.

[33] V Kumar, N Singh, R M Mehra, A Kapoor, L P Purohit, and H C Swart. Role of film thickness on the properties of ZnO thin films grown by sol-gel method. *Thin Solid Films*, 539:161–165, 2013.

[34] K L Foo, M Kashif, U Hashim, and W W Liu. Effect of different solvents on the structural and optical properties of zinc oxide thin films for optoelectronic applications. *Ceramics International*, 40(1):753–761, 2014.

[35] W Chamorro, D Horwat, P Pigeat, P Miska, S Migot, F Soldera, P Boulet, and F Mucklich. Near-room temperature single-domain epitaxy of reactively sputtered ZnO films. *Journal of Physics D: Applied Physics*, 46(23):235107, 2013.

[36] B Abdallah, A K Jazmati, and R Refaai. Oxygen effect on structural and optical properties of ZnO thin films deposited by rf magnetron sputtering. *Materials Research*, 20(3):607–612, 2017.

[37] V Kumar, S K Singh, H Sharma, S Kumar, M K Banerjee, and A Vij. Investigation of structural and optical properties of ZnO thin films of different thickness grown by pulsed laser deposition method. *Physica B: Condensed Matter*, 552:221–226, 2019.

[38] M Mosca, R Macaluso, C Cali, R Butte, S Nicolay, E Feltin, D Martin, and N Grandjean. Optical, structural, and morphological characterisation of epitaxial zno films grown by pulsed-laser deposition. *Thin Solid Films*, 539:55–59, 2013.

[39] D Balzar. Voigt-function model in diffraction line-broadening analysis. *International union of crystallography monographs on crystallography*, 10:94–126, 1999.

[40] J K Saha, R N Bukke, N N Mude, and J Jang. Significant improvement of spray pyrolyzed ZnO thin film by precursor optimization for high mobility thin film transistors. *Scientific Reports*, 10(1):1–11, 2020.

[41] C F Klingshirn, editor. *Zinc Oxide: From Fundamental Properties towards Novel Applications*. Number 120 in Springer Series in Materials Science. Springer, Heidelberg ; London, 2010. ISBN 978-3-642-10576-0.

[42] M Gabas, P Diaz-Carrasco, F Agullo-Rueda, P Herrero, A R Landa-Canovas, and J R Ramos-Barrado. High quality ZnO and Ga: ZnO thin films grown onto crystalline Si (1 0 0) by RF magnetron sputtering. *Solar energy materials and solar cells*, 95(8):2327–2334, 2011.

[43] T G Silva, E Silveira, E Ribeiro, K D Machado, N Mattoso, and I A Hummelgen. Structural and optical properties of ZnO films produced by a modified ultrasonic spray pyrolysis technique. *Thin Solid Films*, 551:13–18, 2014. ISSN 0040-6090. doi: 10.1016/j.tsf.2013.11.011.

[44] D Horwat and A Billard. Effects of substrate position and oxygen gas flow rate on the properties of ZnO:Al films prepared by reactive co-sputtering. *Thin Solid Films*, 515(13):5444–5448, 2007.

[45] M Jullien, D Horwat, F Manzeh, R E Galindo, P Bauer, J F Pierson, and J L Endrino. Influence of the nanoscale structural features on the properties and electronic structure of Al-doped ZnO thin films: An x-ray absorption study. *Solar Energy Materials and Solar Cells*, 95(8): 2341–2346, 2011.

[46] X Zhang, S Ma, F Li, F Yang, J Liu, and Q Zhao. Effects of substrate temperature on the growth orientation and optical properties of ZnO:Fe films synthesized via magnetron sputtering. *Journal of Alloys and Compounds*, 574:149–154, 2013. doi: 10.1016/j.jallcom.2013.04.055.

[47] J Samerkhae, W Maetapa, C Tinnaphob, and T Chanchana. The effects of carrier gas and substrate temperature on ZnO films prepared by ultrasonic spray pyrolysis. *Materials Science in Semiconductor Processing*, 16(3):625–632, 2013.

[48] Mengnan Qu, Jiamin Wu, Guangyu Zhao, and Yuan Zhang. Nanostructured surfaces, coatings, and films: fabrication, characterization, and application, 2013.

[49] S Edinger, N Bansal, M Bauch, R A Wibowo, G Ujvari, R Hamid, G Trimmel, and T Dimopoulos. Highly transparent and conductive indium-doped zinc oxide films deposited at low substrate temperature by spray pyrolysis from water-based solutions. *Journal of Materials Science*, 52(14):8591–8602, 2017.

[50] R C Rai. Analysis of the Urbach tails in absorption spectra of undoped ZnO thin films. *Journal of Applied Physics*, 113(15):153508, 2013.

[51] G Wisz, I Virt, P Sagan, P Potera, and R Yavorskyi. Structural, optical and electrical properties of zinc oxide layers produced by pulsed laser deposition method. *Nanoscale Research Letters*, 12(1):253, 2017.

[52] G X Liang, P Fan, X M Cai, D P Zhang, and Z H Zheng. The influence of film thickness on the transparency and conductivity of Al-doped ZnO thin films fabricated by ion-beam sputtering. *Journal of electronic materials*, 40(3):267–273, 2011.

[53] D Mendil, F Challali, T Touam, A Chelouche, A H Souici, S Ouhenia, and D Djouadi. Influence of growth time and substrate type on the microstructure and luminescence properties of zno thin films deposited by rf sputtering. *Journal of Luminescence*, 215:116631, 2019.

[54] A Kolodziejczak-Radzimska, E Markiewicz, and T Jesionowski. Structural characterisation of ZnO particles obtained by the emulsion precipitation method. *Journal of Nanomaterials*, 2012, 2012. doi: 10.1155/2012/656353.

[55] S Gayathri, O S N Ghosh, S Sathishkumar, P Sudhakara, J Jayaramudu, S Sinha Ray, and K Viswanath. Investigation of physicochemical

properties of Ag doped ZnO nanoparticles prepared by chemical route. *Applied Science Letters*, 1:8, 2015.

[56] Y Li, Y Liu, Z Liu, X Xie, and E C Lee. Improvement of inverted organic solar cells using acetic acid as an additive for zno layer processing. *AIP Advances*, 8(2):025204, 2018.

Declaration of interests

☒ The authors declare that they have no known competing financial interests or personal relationships that could have appeared to influence the work reported in this paper.

☐The authors declare the following financial interests/personal relationships which may be considered as potential competing interests: